Decomposition Rate of a Phenolic Resin

WILLIAM M. BISHOP*
University of Illinois at Urbana-Champaign, Urbana, Ill.

AND

W. J. MINKOWYCZ†
University of Illinois at Chicago Circle, Chicago, Ill.

A test procedure and method of analysis is presented, whereby the overall decomposition rate of the phenolic binder in a silica-phenolic ablator may be separated into its component reactions. The Arrhenius rate equations for these separate reactions are then determined and a reaction mechanism is postulated which predicts the decomposition rate of the phenolic for both constant and varying test temperatures. To the best of the authors' knowledge, this is the first theory which accurately describes the decomposition rate of phenolic resin, and the method should be applicable to other highly cross-linked polymers.

Introduction

PHENOLIC resin is a material widely used as a matrix or binder in heat shield ablatives and is among the most important materials used in commercial industry.[1] At high temperatures, phenolic resin decomposes and thereby affects the over-all strength and thermal conductivity of the material. In particular, it has been shown that depth of charring strongly influences the response of an ablative material to aerodynamic shear effects.[2] Previous attempts to predict the decomposition rates of phenolics have usually assumed single reactions of first order. More realistic approaches have attempted to match thermogravimetric test data with a number of reactions of varying orders.[3,4]

These latter methods will reasonably reproduce test data, but their validity is suspect for heating rates outside of the test range, or for long soak periods. The method presented here actually measures the rates of individual reactions taking place and uses these to predict total weight loss. Although this theory has been developed in connection with an ablative material, the results are not significantly influenced by the silica matrix and should be readily adaptable to commercial applications.

Experimental Work

Two basic types of tests were performed. In the first, the sample was heated at a constant rate of temperature increase from room temperature to the constant temperature level at which reaction rates were to be measured. In the second type of test, the sample was heated at a constant rate up to 1073°K at which point virtually all of the pyrolyzation had ceased. The first type of test is best suited for the data reduction technique to be discussed. The second type is useful in confirming theoretical predictions. The advantage of the constant heating rate is that it minimizes nonequilibrium effects and simplifies the mathematical integration to obtain net weight loss for the varying temperature portion of the test.

The test samples were powdered silica-phenolic, approximately 71/30 silica/Sc-1008 phenolic resin, weighing 250 mg. Humidity was not controlled and the samples may have contained varying amounts of moisture. Thermogravimetric analysis was performed in a Bensen-Lerner furnace using a porcelain crucible. The test atmosphere was either argon or helium with a flow rate of one ft^3/hr.

Sample temperatures were measured by a 0.005 in. diam chromel-alumel thermocouple placed directly over the test sample. For the constant temperature portion of the tests, maximum temperature difference within the slab was estimated to be less than 10^{-2}°K. Temperature difference between the sample surface and the environment was estimated to be less than 2°K for helium, 17°K for argon. Temperature differences during the increasing temperature portion of the tests should be slightly greater, depending upon the heating rate.

Analysis of Constant Temperature Decomposition

Consider a system of q components $W_1, W_2, \ldots, W_q$, where W represents the weight of each component. The general solution[5] for any combination of first-order reactions occurring between these components at any time t is given as

$$W_m = \sum_{j=1}^{q} a_{mj} e^{-\lambda_j t} + \theta_m \tag{1}$$

where m may refer to any individual component; θ_m is a constant of integration representing the weight left at $t = \infty$, and a_{mj} and λ_j are constants determined by the actual reaction rates. The combined weight of all the components may be written as

$$\sum_{m=1}^{q} (W_m - \theta_m) = \sum_{j=1}^{2q} a_j e^{-\lambda_j t} \tag{2}$$

where

$$\sum_{j,m}^{q} \text{ has been written as } \sum_{j}^{2q}$$

The right-hand side of Eq. (2) has the same mathematical form as that for a sum of $n = 2q$ *independent* reactions, where a_j may be considered the initial component weights W_{oj}, and λ_j become the individual reaction rates k_j. The important and useful point made here is that starting with any system of first-order reactions, i.e., competitive, consecutive, etc., these can be expressed as a sum of *independent* reactions, or by analogy with Eq. (2)

$$\sum_{j=1}^{n} W_j = \sum_{j=1}^{n} W_{oj} e^{-k_j t} \tag{3}$$

where it is understood that the W_j may not represent individual component weights. Equation (3) is a marked simplification over the results presented in Eq. (1), and we may now proceed to treat this complex system as the simple system represented by Eq. (3).

Received October 14, 1971; revision received July 28, 1972.
Index categories: Material Ablation; Thermochemistry and Chemical Kinetics.

* Research Assistant, Department of Mechanical and Industrial Engineering.
† Associate Professor, Department of Energy Engineering.

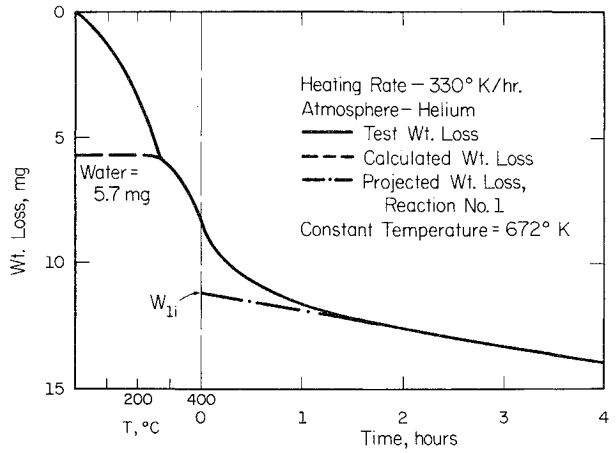

Fig. 1a Test No. 1, weight loss vs temperature and time.

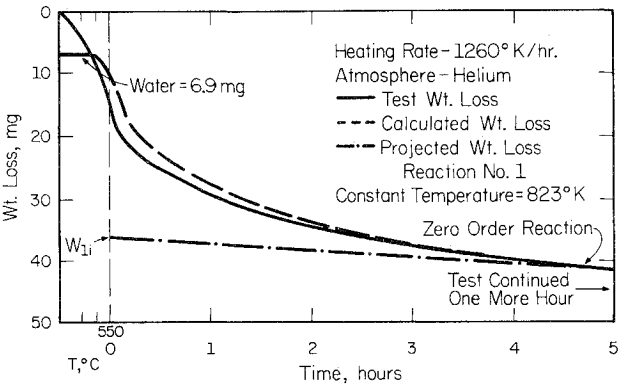

Fig. 2a Test No. 2, weight loss vs temperature and time.

Taking the natural logarithm of Eq. (3) and differentiating the result with respect to time gives

$$\frac{d}{dt}\left(\ln \sum_{j=1}^{n} W_j\right) = \sum_{j=1}^{n} -k_j W_{oj} e^{-k_j t} \Big/ \sum_{j=1}^{n} W_{oj} e^{-k_j t} \tag{4}$$

If the k_j's in Eq. (4) are now arranged in descending order such that $k_1 > k_2 > \cdots > k_n$, we then have

$$e^{-k_1 t} \ll e^{-k_2 t} \ll \cdots \ll e^{-k_n t}$$

and for t large, Eq. (4) reduces to

$$\frac{d}{dt}\left(\ln \sum_{j=1}^{n} W_j\right) = -k_n \tag{5}$$

Thus, for long test times, the plot of the logarithm of the total weight of a complex, first-order system vs time reduces to a straight line, the slope of which is the negative of the lowest value of k_j. Further, at large times, the only weight change in Eq. (5) is that for the weight associated with k_n, namely, W_n, or

$$d(\ln W_n) = -k_n\, dt \tag{6}$$

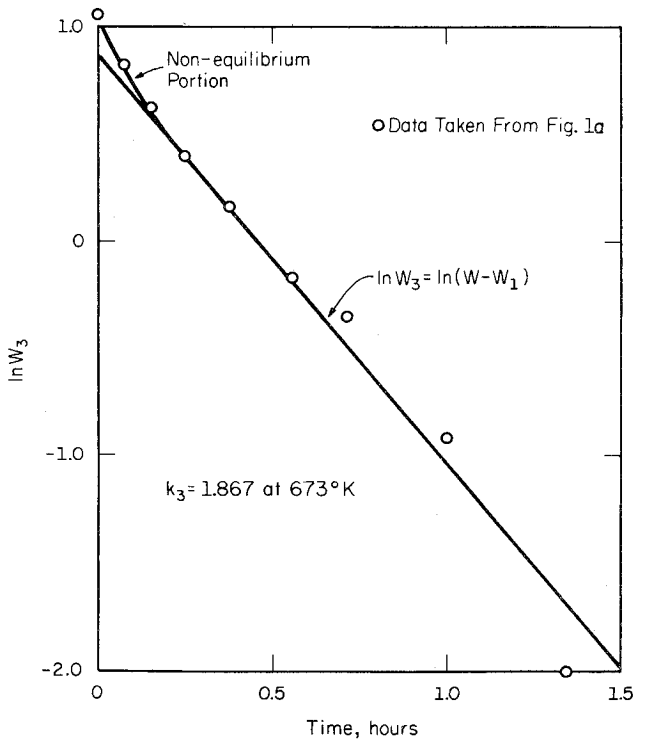

Fig. 1b Ln W_3 vs time at 673°K.

Integrating Eq. (6) gives

$$\ln W_n = \ln W_{on} - k_n t \tag{7}$$

where W_{on} is the apparent initial weight of component n. Ln W_{on} may be obtained by extrapolating the straight line ln W_n vs t back to $t = 0$. It is now possible to calculate $W_n(t)$ using Eq. (7). Subtracting $W_n(t)$ from the composite weight history [Eq. (3)] and plotting the logarithm of this remaining weight vs time once again gives a straight line for t large, the slope of which is $-k_{n-1}$. This process may be continued until the rate constants and initial weights have been determined for each W_j. The only requirement is that the complex system be of first order. In the high pressure limit, gas phase decomposition reactions are typically of first order and it is not unreasonable to expect the same situation for solid phase decomposition.

Application of Constant Temperature Analysis to Test Results

Results of Tests 1, 2, and 3 shown in Figs. 1a, 2a, and 3a consist of 250 mg samples brought to temperatures of 673°K, 823°K, and 923°K, respectively, and held at these temperatures for several hours. These tests were analyzed in the manner described and logarithmic straight line results depicting the reaction rates k_n are presented in Figs. 1b, 2b, 2c, 3b, and 3c, respectively. The measured rates for each test are presented in tabular form as a function of temperature (see Table 1).

Note that Reaction No. 1 behaves kinetically as a zero-order reaction; that is, the weight loss appears independent of the amount of reactant available and is a straight line on the constant temperature weight loss histories. This reaction, probably at least second- or third-order[6] takes place between the silica and the carbon residue of the phenolic at the surface of the silica fibers. Gas chromatograph analysis shows the product to be carbon monoxide. Note also that Reaction No. 2 does not take place in Test No. 1 due to the low test temperature. This is discussed later.

Since the k_n's actually represent individual eigenvalues for the

Table 1 Experimentally determined rate constants

Test No.	T(°K)	k_1, hr^{-1}	k_2	k_3	k_4
1	673	0.700	[a]	1.867	8.12
2	823	0.972	0.668	4.468	13.00
3	923	1.124	0.945	6.860	[a]

Reaction No.	B, °K	ln A	A, hr^{-1}
1	1.176×10^3	1.389	4.01
2	2.620×10^3	2.778	16.1
3	3.210×10^3	5.397	221
4	1.770×10^3	4.725	113

[a] Not observed.

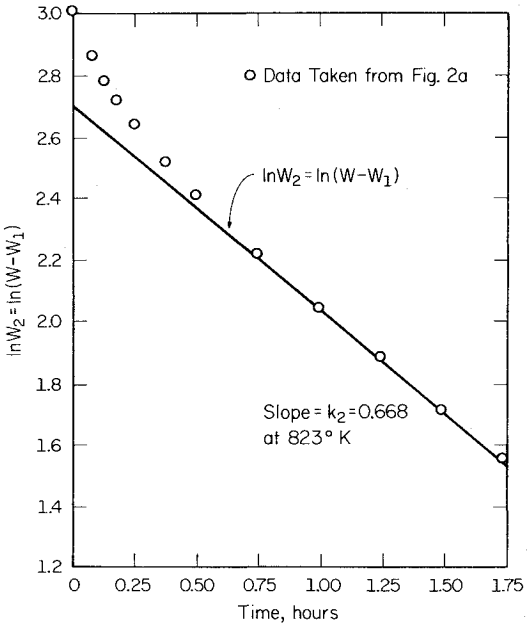

Fig. 2b Ln W_2 vs time at 823°K.

complex system as demonstrated in Eqs. (2) and (3), they should satisfy the Arrhenius rate equation

$$\ln k = \ln A - B/T \tag{8}$$

Thus the logarithms of the individual k's, when plotted vs the inverse of temperature, should form a straight line. Such a plot is shown in Fig. 4. For those reactions for which three data points (rates) are available (Reactions No. 1 and 3), agreement with Eq. (8) is excellent. Reaction No. 2, for which there are only two data points, is based on large weight losses (see Figs. 2 and 3); its accuracy can be determined from the fact that the weight loss

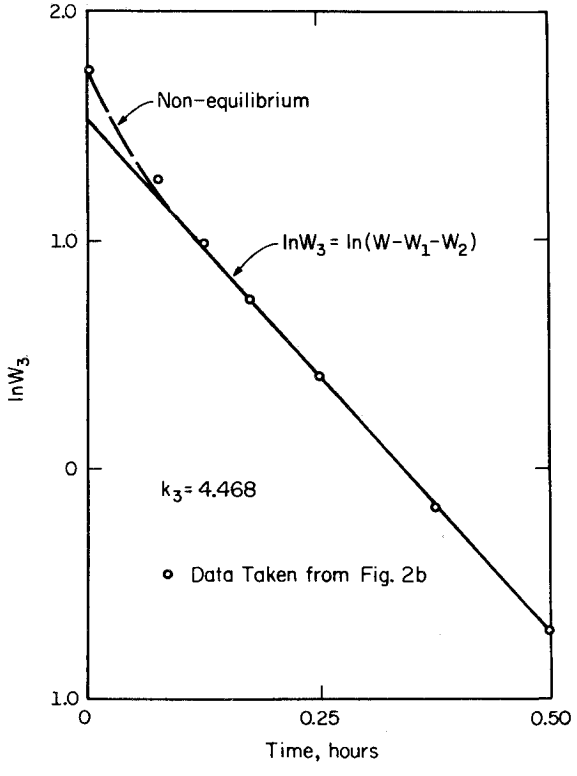

Fig. 2c Ln W_3 vs time at 823°K.

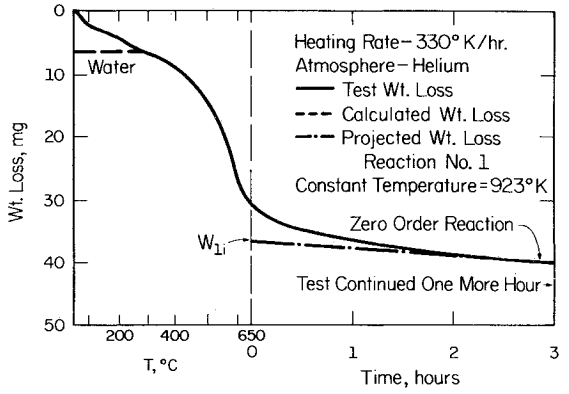

Fig. 3a Test No. 3, weight loss vs temperature and time.

histories at constant temperature are reproducible by its use. Reaction No. 4 occurs at the point where the tests change from constant heating rate to constant temperature and is considered to be a nonequilibrium effect, especially since no weight loss of the magnitude predicted by this reaction occurs in the tests. This nonequilibrium effect is particularly noticeable in the high heating rate tests and will be discussed further. For the sake of brevity, ln W_4 vs time curves are not presented. It should be noted that rate constants determined from the test data can be correlated with specific reactions only by observing which straight line they fall on in Fig. 4. The relatively small number of reactions seen compared with the decomposition products observed by gas chromatograph indicate that many reactions take place in the gas phase after decomposition has taken place. Naturally, this does not affect the mass loss rate.

Using Fig. 4 and Eq. (8), it is now possible to obtain the Arrhenius rate constants A and B for each of the reactions. These

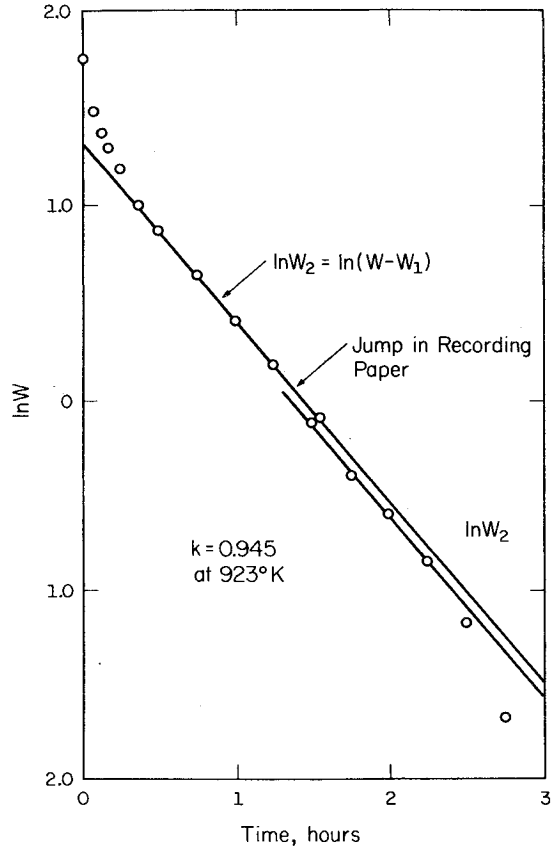

Fig. 3b Ln W_2 vs time at 923°K.

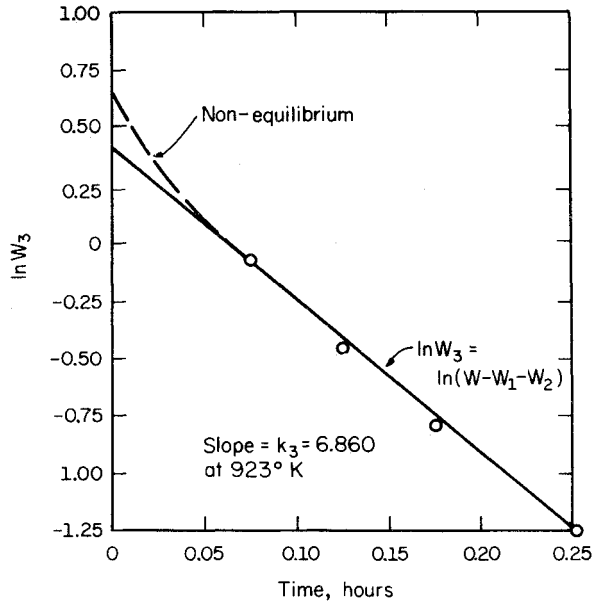

Fig. 3c Ln W_3 vs time at 923°K.

constants are presented in Table 1. It still remains to determine the initial amounts of reactants actually present in the virgin material at room temperature. This requires integrating the three separate reactions from the start of the constant temperature range, back over the constant heating rate test range, to room temperature. The method of integration used for this purpose was originally presented in 1962 in an unpublished report by T. R. Munson[7] of Avco Corp. and is discussed next.

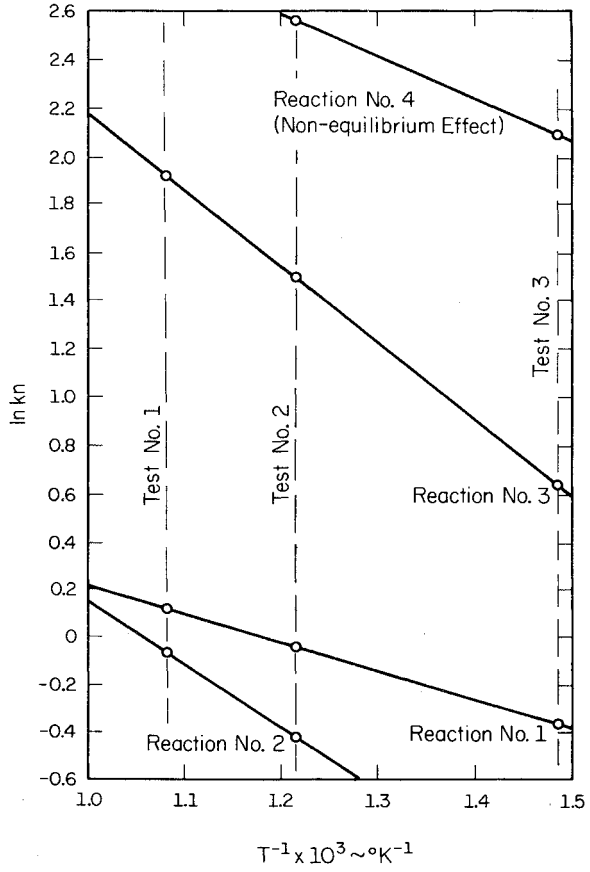

Fig. 4 Ln k_n vs T^{-1}, tests 1, 2, and 3.

Analysis of Variable Temperature Decomposition

The original derivation is valid for all orders of reaction. The first- and zero-order derivations are presented here for the convenience of the reader.

The reaction rate for a first-order reaction is given by

$$dW/dt = -Wk \tag{9}$$

Substituting the Arrhenius expression for k gives

$$dW/dt = -WAe^{-B/T} \tag{10}$$

Letting $\beta = dT/dt$ (constant heating rate), $\xi = (T_i/T)$, and integrating Eq. (10) yields

$$\int_{W_o}^{W_i} \frac{dW}{W} = \frac{-AT_i}{\beta} \int_1^{\infty} \frac{\exp[-(B/T_i)\xi]}{\xi^2} d\xi \tag{11}$$

where the upper limit of integration is $\xi = T_i/T_o = \infty$, T_o is the temperature of the substance at the beginning of the experiment, and T_i is the temperature at which it is desired to determine the weight W_i. Since the reaction rates become vanishingly small at T_o (room temperature in this case), this limit may be extended to $T_o = 0$ without affecting the accuracy of the integral. The right-hand side of Eq. (11) is an incomplete gamma function of the form

$$E_2(x) = \int_1^{\infty} \frac{\exp(-X\xi)d\xi}{\xi^2} \tag{12}$$

which is tabulated as a function of the argument in Ref. 8. Thus, Eq. (11) becomes

$$\ln(W_i/W_o) = (-AT_i/\beta)E_2(B/T_i) \tag{13}$$

For the case of the zero-order reaction, there results

$$W_o - W_i = (AT_i/\beta)E_2(B/T_i) \tag{14}$$

Using Eqs. (13) and (14), the three actual reactions may now be integrated from the end of the constant heating rate test portion back to room temperature to obtain the virgin W_o's. For the case of simple independent reactions, the values of W_o for a particular reaction should be equal from test to test. However, only W_o's for Reaction No. 1 (the zero-order reaction) are consistent (214.0 mg). This is not surprising since the phenolic initially does not consist of separate substances. Rather, some solid phase reaction which produces the separate reactants must take place. At this point it is necessary to postulate a specific reaction mechanism which determines the apparent measured rates 2 and 3, assuming that Reaction No. 1 is effectively independent.

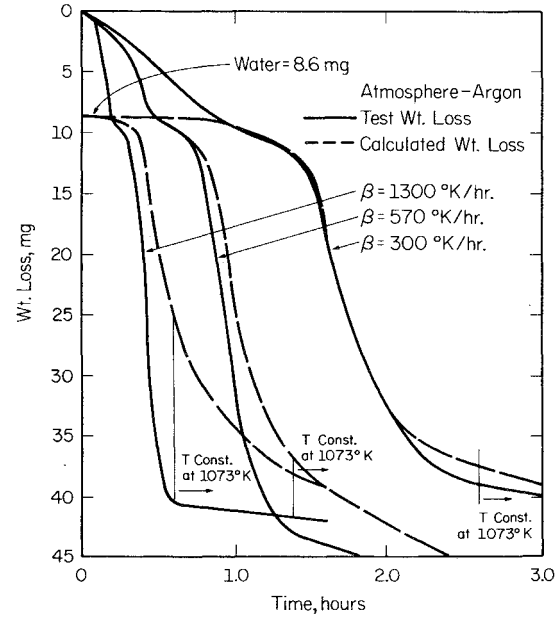

Fig. 5 Weight loss vs time at various heating rates in an argon atmosphere.

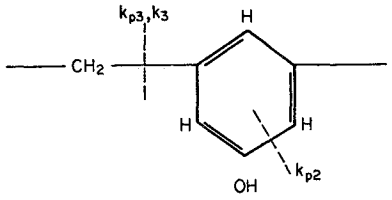

Fig. 6 Postulated modes of decomposition.

A simple mechanism which explains all of the test phenomena is as follows

$$W_p \xrightarrow{k_{p2}} W_2 \xrightarrow{k_2} \text{gas} \tag{15a}$$

$$W_p \xrightarrow{k_{p3}} W_3 \xrightarrow{k_3} \text{gas} \tag{15b}$$

Molecularly, this may be represented by Fig. 6. Here K_{p3} takes place randomly throughout the polymer at the bond indicated. Eventually these breaks produce small groups of more or less cross-linked monomers each connected to the main body of polymer by one bond only. This is W_3. The breaking of this single bond is the reaction k_3 producing a gas. At higher temperatures, the ring itself breaks down as indicated by k_{p2}. This produces W_2 (the broken ring) which decomposes at the rate k_2, eventually leaving a carbon residue. The location given for the initial break, k_{p2}, is purely speculative and may actually be variable. This model is in basic agreement with the qualitative descriptions given by Madorsky[1] and Winslow.[9]

Using the scheme given by Model (15), the total weight of the volatile components of the phenolic for a constant temperature history is given by

$$\begin{aligned} W_p + W_2 + W_3 = {} & \left(W_{2i} - k_{p2}\, W_{pi}/[k_2 - (k_{p2} + k_{p3})]\right) e^{-k_2 t} + \\ & \left(W_{3i} - k_{p3}\, W_{pi}/[k_3 - (k_{p2} + k_{p3})]\right) e^{-k_3 t} + \\ & W_{pi}\{1 + k_{p2}/[k_2 - (k_{p2} + k_{p3})] + \\ & k_{p3}/[k_3 - (k_{p2} + k_{p3})]\}\, e^{-(k_{p2} + k_{p3})t} \end{aligned} \tag{16}$$

where W_{pi}, W_{2i}, and W_{3i} represent the weights of reactants present at the start of the constant temperature decomposition. In the constant temperature portions of Tests 1, 2, and 3, W_{pi} has completely decomposed and the terms containing W_{pi} drop out leaving

$$W_2 + W_3 = W_{2i}\, e^{-k_2 t} + W_{3i}\, e^{-k_3 t} \tag{17}$$

which is identical to the result of the previous constant temperature analysis [Eq. (3)]. For a constantly increasing temperature history, W_p is obtained using Munson's method as

$$W_p(T) = W_{op} \exp\{-T^*/\beta[A_{p2} E_2(B_{p2}/T^*) + A_{p3} E_2(B_{p3}/T^*)]\} \tag{18}$$

where W_{op} is the original weight of W_p available before the onset of decomposition, T is the temperature at which it is desired to find W_p, and T^* is the stable temperature of the phenolic to be discussed later. W_2 and W_3, for a constantly increasing temperature history, may be obtained from Model (15) as

$$W_2 = \int_0^T \frac{1}{\beta}(-A_2\, e^{-B_2/T^*} W_2 + A_{p2}\, e^{-B_{p3}/T^*} W_p)\, dT \tag{19}$$

and

$$W_3 = \int_0^T \frac{1}{\beta}(-A_3\, e^{-B_3/T^*} W_2 + A_{p3}\, e^{-B_{p3}/T^*} W_p)\, dT \tag{20}$$

Equations (19) and (20) must be integrated numerically. Equations (14 and 18–20) completely describe the weight loss history for constant β. Equation (14) employs the measured zero-order rate constants A_1 and B_1, while Eqs. (18–20) employ the measured constants A_2, B_2, A_3, and B_3. The unknown constants A_{p2}, B_{p2}, A_{p3}, and B_{p3} must be determined numerically by fitting Eqs. (18–20) to the weight loss data for constant β tests. A large number of tests were available for this purpose. As noted previously, Test 1 (see Fig. 1) shows that the primary material is stable up to at least 673°K. The actual maximum stable temperature was determined numerically to be approximately 690°K for both k_{p2} and k_{p3} (in reality there is probably a separate stable temperature for each reaction). Thus, the temperature used in Eqs. (18–20) is actually $T^* = T - 690$°K. The use of a stable temperature is not consistent with gas phase decomposition theory[10] where the Arrhenius rate equation is obtained using the energy distribution over all temperatures. This suggests that a more satisfactory approach may be to use the RRK model[11] combined with some simple model for the energy distribution in a solid. The primary rate constants obtained using the above numerical procedure are $A_{p2} = 210\ \text{hr}^{-1}$, $B_{p2} = 300$°K, $A_{p3} = 10\ \text{hr}^{-1}$, and $B_{p3} = 22$°K. These constants are necessarily approximate since the weight losses measured are determined mainly by the integrated primary reaction rates, not the rates themselves.

It is now possible to calculate weight loss history over the whole range of test conditions, using the appropriate equations for the constant β and constant T test portions. Weight loss for arbitrary temperature histories may be handled numerically.

The validity of the reaction mechanism presented in Eq. (15) can only be checked by its reproduction of the test data. The uniqueness of Eq. (15) is demonstrated by the fact that no other simple mechanism incorporating the observed reactions will reproduce the data. Taking Reaction No. 1 to be between the carbon residue and the silica matrix leaves only two observed reactants, W_2 and W_3, which must be derived from the primary material W_p. There are only five first-order reaction schemes (excluding nonrate controlling intermediate steps) which will produce the correct number of reactions. Of these, only the scheme represented by Eq. (15) satisfies the weight loss data using the measured rates.

The amount of W_3 appears to depend upon cleavage caused by powdering the sample as well as upon temperature. Test 1 (see Fig. 1b) shows a portion of preformed W_3 (3.8 mg) which decomposes initially before the primary decomposition stable temperature has been exceeded. This percentage (12.9% of weight after subtraction of W_{01} and water) of preformed W_3 was assumed constant for each of the samples and was treated separately in the calculations using the reaction rate k_3. No solid sample tests were available to check this idea. Also, solids tend to produce large transient effects which is another problem.

Discussion of Results

The calculated weight histories for the original three tests are represented by the dashed lines in Figs. 1a, 2a, and 3a. Additional test results are compared with theory in Fig. 6. In the latter tests the atmosphere was argon, and for the lower rate tests there is a well defined plateau in the weight loss history at about 600°K and approximately 8.6 mg weight loss. This plateau represents the point where all of the absorbed water has been removed and the phenolic has not yet started to decompose. In the helium atmosphere tests, this plateau is not as well defined. No constant temperature tests were available to the authors at the water loss temperature level, and a prediction of this portion of the history was not attempted. Indeed, substances other than water may be involved here.

Agreement of theory with test weight loss is excellent for all of the low heating rate tests (350°K/hr). Agreement lessens as the heating rate increases, and is poor for the high rates (1300°K/hr) where the weight loss is much faster than predicted. In fact, the fastest reaction observed in the constant temperature tests will not predict this weight loss even if all the initial weight is allocated to it. Moreover, Test 2, which has a high heating rate, satisfies predictions exactly once the temperature becomes constant (as do all of the tests). Thus, this excess weight loss is considered to be a nonequilibrium effect, probably a secondary combustion reaction, the escaping interior gases reacting with the higher temperature outer residue and increasing its rate of decomposition. This effect could be minimized in future tests by making the sample as close to an infinitely thin sheet as possible. However,

since secondary reactions will undoubtedly be present in most practical applications, an ability to predict their rates is desirable. The secondary reaction rates, in general, will be controlled by the temperature of the outer residue. Depending on this temperature, the reaction(s) will either be diffusion or reaction rate controlled.

Finally, the reaction rates k_1 for tests in Fig. 6 do not agree exactly with those predicted. Measured rates dW_1/dt for those tests at 800°C (not shown on figures) are 1.7, 2.0, and 1.2 mg/hr, respectively, vs a calculated value of 1.35 mg/hr for a remaining sample weight of approximately 205 mg. These samples are from different manufacturers, have different ratios of silica to phenolic, and it is probable that the surface area of the silica fiber varies for each sample. In view of the extremely small rates involved and the secondary nature of the reaction, no correction to these rates was attempted.

An attempt was made to compare Madorsky's[1] experimental results with the present theory. All of Madorsky's tests are at or below the stable temperature of the phenolic, leaving only the preformed W_3 as a possible reactant (assuming no absorbed water). The amount of preformed W_3 depends upon the degree of cure and powdering of the sample. Also, in Madorsky's tests, samples were inserted into a preheated furnace as opposed to gradual heating. With these differences in mind, comparison with theory was good at the high temperature range (2.5%/hr vs 3.2% calculated at 420°C) and poor at the lower temperatures (factor of 5 to 10 differences). The poor agreement at low temperature is thought to be due to the fact that W_3 must approach a stable temperature in this range, as it is stable at room temperature. For tests with a relatively high constant heating rate, as presented in this paper, the weight loss in this range is too small to warrant use of this stable temperature.

Conclusions

The prediction method presented appears satisfactory for low heating rates and for long soak times. At high heating rates, minimum losses are predicted only, due to secondary reactions. This requires additional study. Further tests should be made in the primary reaction temperature range to investigate possible application of the RRK model. In so far as the method has proved successful in the prediction of phenolic weight losses, it should also now be possible to accurately measure the heats of reaction associated with each reactant. Application of the method to other solid polymers will probably involve postulation of mechanisms other than that given by Eq. (15). The decomposition of wood and coal may also lend itself to this approach. Since all tests were conducted at atmospheric pressure, it was not possible to measure the effect of pressure on decomposition rate. However, considering the nature of the reactions, namely decomposition (as opposed to sublimation) from a solid to a gas, it is unlikely that variation in pressure will significantly affect decomposition rates.

Referemces

[1] Madorsky, S. L., *Thermal Degradation of Organic Polymers*, Interscience, New York, 1964, Chap. XVI.

[2] Bishop, W. M. and DiCristina, V., "A Prediction Technique for Ablative Material Performance under High-Shear Re-Entry Conditions," *AIAA Journal*, Vol. 6, No. 1, Jan. 1968, pp. 59–63.

[3] Nelson, J. B., "Determination of Kinetic Parameters of Six Ablation Polymers by Thermogravimetric Analysis," TN D-3919, April 1967, NASA.

[4] Munson, T. R., Mascola, R. E., Brown, J. D., Spindler, R. J., and Klugerman, J., "An Advanced Analytical Program for Charring Ablators," AVSSD-0172-67-RR, Vol. 1, 1967, Avco Space Systems Div., Lowell, Mass.

[5] Bensen, S. W., *The Foundation of Chemical Kinetics*, McGraw-Hill, New York, 1960, pp. 39–42.

[6] Beecher, N. and Rosenweig, R. E., "Ablation Mechanisms in Plastics with Inorganic Reinforcement," *ARS Journal*, Vol. 31, April 1961, pp. 532–539.

[7] Munson, T. R., 'Thermal Decompositon Kinetics of Polymeric Materials," TA-1057, Feb. 1962, Avco Systems Div., Wilmington, Mass.

[8] *Tables of Functions and Zeros of Functions*, AMS37, National Bureau of Standards, Government Printing Office, Washington, D.C., 1954.

[9] Winslow, F. H., Baker, W. O., Pape, N. R., and Matreyek, W., "Formation and Properties of Polymer Carbon," *Journal of Polymer Science*, Vol. 16, No. 82, April 1955, pp. 101–120.

[10] Slater, N. B., *Theory of Unimolecular Reactions*, Cornell University Press, New York, 1959, Chap. 2.

[11] Kassel, L. S., *The Kinetics of Homogeneous Gas Reactions*, The Chemical Catalog Co., New York, 1932, Chap. V.